Functional paclitaxel plus honokiol micelles destroying tumour metastasis in treatment of non-small-cell lung cancer

Xin Wang, Lan Cheng, Hong-Jun Xie, Rui-Jun Ju, Yao Xiao, Min Fu, Jing-Jing Liu & Xue-Tao Li

Published online: 25 Jul 2018.

Submit your article to this journal ☐

View related articles ☐

View Crossmark data ☐

Taylor & Francis
Taylor & Francis Group

Check for updates

Functional paclitaxel plus honokiol micelles destroying tumour metastasis in treatment of non-small-cell lung cancer

Xin Wang[a], Lan Cheng[a], Hong-Jun Xie[b], Rui-Jun Ju[c], Yao Xiao[a], Min Fu[a], Jing-Jing Liu[a] and Xue-Tao Li[a]

[a]School of Pharmacy, Liaoning University of Traditional Chinese Medicine, Dalian, China; [b]Medical School, Tibet University, Lasa, China; [c]Department of Pharmaceutical Engineering, Beijing Institute of Petrochemical Technology, Beijing, China

ABSTRACT

Treatment effect of chemotherapy for aggressive non-small-cell lung cancer (NSCLC) is usually unsatisfactory for non-selective distributions of anticancer drugs, generation of vasculogenic mimicry (VM) channels, high metastasis and recurrence rate. Therefore, we developed a kind of dequalinium (DQA) modified paclitaxel plus honokiol micelles in this study to destroy VM channels and inhibit tumour metastasis. *In vitro* assays indicated that the targeting paclitaxel micelles with ideal physicochemical characteristics could exhibit not only the powerful cytotoxicity on Lewis lung tumour (LLT) cells but also the effective suppression on VM channels and tumour metastasis. Action mechanism studies manifested that DQA modified paclitaxel plus honokiol micelles could activate apoptotic enzymes caspase-3 and caspase-9 as well as down-regulate FAK, PI3K, MMP-2 and MMP-9. *In vivo* assays indicated that polymeric micelles could increase selective accumulation of chemotherapeutic drugs at tumour sites and showed a conspicuous antitumour efficacy. Hence, the DQA modified paclitaxel plus honokiol micelles prepared in this study provided a potential treatment strategy for NSCLC.

Introduction

Lung cancer is a malignant tumour characterized by the uncontrolled cell growth in lung [1]. This growth can spread beyond the lung by process of metastasis into nearby tissues or other parts of the body [2]. At present, lung cancer is the most common cause of cancer-related death in men and the second most common in women. According to the pathological features, lung cancer can be generally divided into small-cell lung carcinoma (SCLC) and non-small-cell lung carcinoma (NSCLC). NSCLC is a kind of frequently occurring lung cancer and accounts for about 85% of all lung cancers [3]. Usually, the traditional treatments for NSCLC include surgery, radiation therapy and chemotherapy, and the treatment effect depends on the stage of cancer, the individual's overall health and the side effects of treatment. Surgery is only successfully used to cure the patients who are diagnosed with the early stage of NSCLC and the cancer cells have not spread beyond nearby lymph nodes [4]. Although chemotherapy is often used in patients who are not eligible for surgery, the treatment effect is usually unsatisfactory for the non-selective distributions of anticancer drugs, the generation of vasculogenic mimicry (VM) channels and the high metastasis of cancer cells [5].

VM channels, first described in uveal melanomas by Maniotis in 1999, are the formation of microvascular channels directly generated from aggressive, metastatic and genetically deregulated cancer cells under hypoxia [6]. VM channels could accelerate tumour metastasis and provide adequate nutrition for the rapid growth of tumours. It was reported that the poor prognosis of lung cancer patients was closely related to the formation of VM channels [7–9]. Metastasis is the spread of cancer cells from an initial or primary site to a different or secondary site. The spread of metastasis may occur via blood or lymphatic and metastatic tumours are very common in the late stages of cancer [10]. Metastasis is the primary challenge for cancer treatment with a multifactorial process involving multiple signalling molecules from different signalling pathways. An increasing number of studies had indicated that the inhibition of cancer cells metastasis could remarkably enhance therapeutic effects for NSCLC [11–13].

Dequalinium (DQA) is a quaternary ammonium cation. As a kind of mitochondrial-targeted drug, DQA can selectively accumulated in the mitochondria of cancer cells. Some previous studies had demonstrated that the modification of DQA on the liposomal surface could increase the cellular uptake by electrostatic interactions [14,15]. Honokiol is an active natural extract of traditional Chinese herb *Magnolia offcinalis*, and it is widely used as a supplementary functional drug in treatment of cancer for the various biological properties such as inhibiting the VM channels, suppressing the invasion of cancer cells and reducing the adhesion rate between cancer cells and body environment [16,17]. Paclitaxel is one of the most effective chemotherapy drugs for treating various kinds of cancer. The underlying mechanism for the cytotoxicity of paclitaxel is mainly from binding tubulin and stabilizing microtubules. These stable microtubules inhibit the division

of cancer cells at the G2/M phase of cell cycle [18,19]. Therefore, the combination of paclitaxel plus honokiol was considered for the preparation of micelles. In this way, the proliferation of lung cancer cells was restricted by paclitaxel, and cellular metastases and VM channels were suppressed by honokiol in the meanwhile. This combination fundamentally solved the problem of tumor metastasis which was inevitable for traditional chemotherapy when killing cancer cells.

Among the emerging drug delivery systems, nanomicelles system is one of the most promising approach to improve the solubility of hydrophobic drugs in the body [20]. Polyvinyl caprolactam-polyvinyl acetate-polyethylene glycol graft copolymer (Soluplus) is a graft amphiphilic copolymer with a low critical micelle concentration (0.76×10^{-3}% w/v), and it is enable to form the nanomicelles system with good solubility for hydrophobic drugs [21]. D-alpha-Tocopheryl polyethylene glycol 1000 succinate ($TPGS_{1000}$) is a derivative of vitamin E that can directly enhance the bioavailability of poorly soluble actives, and it is widely used as an emulsifier, solubilizer, bioavailability enhancer and a vehicle for a lipid-based drug formulation [22].

In the present study, we hypothesized that the targeting paclitaxel plus honokiol nanomicelles modified with DQA could inhibit the formation of VM channels, suppress the cancer cells metastasis and then target to cancer cells. In this construction, soluplus and $TPGS_{1000}$ are used as basic material to form nanomicelles, DQA was modified on the surface of the micelles for specifically binding to cancer cells, honokiol was incorporated into the micelles for inhibiting the VM channels and cancer cells metastasis, and paclitaxel was encapsulated into micelles as anticancer drugs. The aim of this study is to create the DQA modified paclitaxel plus honokiol nanomicelles, evaluate the anticancer effects and clarify the relevant mechanism.

Materials and methods

Reagents and cell lines

Soluplus was provided by Fengli Jingqiu Pharmaceutical Co., Ltd. (Beijing, China). $TPGS_{1000}$ and DQA were purchased from Sigma-Aldrich (Saint Louis, MO, USA). Paclitaxel and honokiol were purchased from Meilun Biotechnology Co., Ltd. (Dalian, China). Polyethylene glycol-distearoyl phosphatidylethanol-amine-NHS (DSPE-PEG_{2000}-NHS) was purchased from NOF Corporation (Tokyo, Japan). Dulbecco's modified eagle medium (DMEM) medium and foetal bovine serum (FBS) were ordered from GIBCO (Billings, MT). Lewis lung tumour (LLT) cells were obtained from the Institute of Basic Medical Science, Chinese Academy of Medical Science (Beijing, China), and incubated in DMEM supplemented with 10% FBS and 1% antibiotics (100U/mL penicillin, and 100 μg/mL streptomycin) under an atmosphere of 5% CO_2 at 37 °C. Other chemicals were analytical or high-performance liquid chromatography (HPLC) grade. C57BL/6 mice (18–20 g) were purchased from Liaoning Changsheng Biotechnology Co., Ltd. (Benxi, China). All procedures were performed according to guidelines of the Institutional Authority for Laboratory Animal Care of Liaoning University of Traditional Chinese Medicine.

Synthesis of targeting molecule

The targeting molecule was produced by an acylation reaction [23]. That is, the amino group on DQA was reacted with the NHS group on DSPE-PEG_{2000}-NHS. To prove the successful synthesis of targeting molecule, DSPE-PEG_{2000}-DQA was measured and characterized using a matrix-assisted laser desorption/ionization-time-of-flight mass spectrometry (MALDI-TOF-MS, Bruker Daltonics, Bremen, Germany). Briefly, DSPE-PEG_{2000}-NHS was blended with DQA at 1:1 molar ratio in anhydrous dimethylformamide and then regulated the pH to 9 by means of moderate N-methylmorpholine. After 24 h of stirring at room temperature, the solution was dialyzed against distilled water once every 12 h (2 times) to remove the uncombined molecules. Then, the resultant was analyzed by MALDI-TOF-MS.

Preparation of micelles

Micelles were prepared by film dispersion method and the composition of DQA modified paclitaxel plus honokiol micelles was soluplus, $TPGS_{1000}$, DSPE-PEG_{2000}-DQA, paclitaxel and honokiol with the mass ratio of 100:25:6:1:1 [24]. Briefly, all materials were blended in a round-bottom flask and dissolved in methanol, and the flask was kept under vacuum at 40 °C by a rotary evaporation to remove the methanol. A transparent film was formed on the inner wall of the flask. After the flask was cooled, the transparent film was dissolved with the right amount of PBS buffer (pH 7.4) and shaken for 20 min to promote the formation of micelles. Then, the micelles were extruded through microporous membranes with pore size of 0.22 μm for 2 times and the DQA modified paclitaxel plus honokiol micelles were obtained.

Blank micelles, paclitaxel micelles, honokiol micelles, DQA modified paclitaxel micelles and paclitaxel plus honokiol micelles were prepared according to the same method, and the compositions were soluplus/$TPGS_{1000}$/DSPE-PEG_{2000}-DQA (100:25:6, mass ratio), soluplus/$TPGS_{1000}$/paclitaxel (100:25:1, mass ratio), soluplus/$TPGS_{1000}$/honokiol (100:25:1, mass ratio), soluplus/$TPGS_{1000}$//DSPE-PEG2000-DQA/paclitaxel (100:25:6:1, mass ratio) and soluplus/$TPGS_{1000}$/paclitaxel/honokiol (100:25:1:1, mass ratio), respectively. Besides, coumarin micelles, coumarin plus honokiol micelles, DQA modified coumarin plus honokiol micelles (lipids/coumarin = 100:1, w/w), DiR micelles and DQA modified DiR plus honokiol micelles (lipids/DiR = 200:1, w/w) were similarly prepared as fluorescence probes for demonstrating the micellar distribution *in vitro* and *in vivo*.

Characterization of the micelles

The morphology of DQA modified paclitaxel plus honokiol micelles was observed by a transmission electron microscope (TEM; Tecnai G2 20ST; FEI Co., Tokyo, Japan). Particle size and polydispersity index (PDI) were further measured by a Nano Series Zen 4003 Zetasizer (Malvern Instruments Ltd., Malvern, UK). To measure the encapsulation efficiencies (EE) of paclitaxel and honokiol, the micelles were demulsified by adding methanol. After centrifugation for 15 min, the supernatant

was analysed by HPLC equipped with a UV detector (Shimadzu, LC-2010 AHT, Japan). The encapsulation efficiency was calculated using the formula: $EE\% = (W_{encap}/W_{total}) \times 100\%$, where W_{total} and W_{encap} were the amount of drug added in the micellar suspensions and the amount of drug measured by HPLC, respectively. The release behaviours of paclitaxel and honokiol from micelles in PBS solution containing 10% FBS were analysed by dialysis according to our previous report [23]. In short, the varying micelles were plus with equal volume of PBS solution containing 10% FBS, and then were filled into the dialysis bags (MW cut-off = 12,000–14,000 Da). The dialysis bags were immersed into PBS solution and oscillated by gentle shaking (100 rpm) at 37 °C. Then, 0.5 ml release medium was sampled at 6, 12, 24 and 48 h, followed by adding the same amount of fresh release medium after each sampling. The content of paclitaxel or honokiol in samples was analysed by the HPLC. The release rate (RR) of paclitaxel or honokiol was calculated using the following formula: $RR\% = (W_i/W_t) \times 100\%$, where W_i and W_t referred to the amount of drug in the release medium at different time-point measured by HPLC and the amount of drug encapsulated in the micelles, respectively.

Cytotoxic effects on LLT cells

A sulforhodamine B (SRB) staining method was used to evaluate the cytotoxic effects of varying micellar formulations on LLT cells according to our previous report [25]. Briefly, LLT cells were seeded in 96-well culture plates (1×10^4 cells/well) and incubated at 37 °C for 24 h. Stale medium was removed and cells were washed 2 times with PBS buffer. In free drug treatment groups, fresh DMED medium containing different concentrations of free drug was added into the wells, including free paclitaxel, free honokiol and the mixture of the two drugs at different proportions. The concentrations of paclitaxel were in the range of 0–5.0 μM, and the ratio of paclitaxel to honokiol was 1:0.5, 1:1, and 1:3, respectively. To evaluate the synergistic effect of paclitaxel plus honokiol, combined index (CI) of drugs was calculated by the following formula: $CI = a/A + b/B$, where "a" and "b" are the IC_{50} values of the two drugs used conjunctively, and "A" and "B" are the IC_{50} values of the two drugs used alone. The smaller CI value represents the stronger synergy between paclitaxel and honokiol. In micelle treatment groups, LLT cells were treated with blank micelles, paclitaxel micelles, DQA modified paclitaxel micelles, paclitaxel plus honokiol micelles and DQA modified paclitaxel plus honokiol micelles, respectively. The concentration of paclitaxel was in the range of 0–10 μM (paclitaxel/honokiol = 1:1, mass ratio). After incubations for 48 h, LLT cells were fixed with 10% trichloroacetic acid and stained with 0.4% SRB dye. Then, Tris base solution was added to dissolve the combined dye. Finally, the optical densities were measured by a microplate reader (HBS-1096A; DeTie Laboratory Equipment, Nanjing, China) at 540 nm. The survival rates of LLT cells were calculated using the following formula: survival % = (A540 nm for treated cells/A540 nm for control cells) × 100%, where A540 nm represented the absorbance value measured at 540 nm. Dose-effect curves were plotted and IC_{50} values were calculated using GraphPad Prism software Version 6.0 (GraphPad Software Inc., La Jolla, CA). Three duplicate wells were set up for each group.

Cellular uptake and targeting effects in LLT cells

Coumarin was encapsulated in the micelles as fluorescent probe to observe the cellular uptake and targeting effects in LLT cells. Briefly, LLT cells were seeded in 6-well culture plates at a density of 4×10^5 cells per well and incubated at 37 °C for 24 h. Then, the cells were incubated with the medium containing the varying micellar formulations at a concentration of 2 μM coumarin, including coumarin micelles, DQA modified coumarin micelles, coumarin plus honokiol micelles and DQA modified coumarin plus honokiol micelles, respectively. Blank micelles was used as blank control. After incubation for 3 h, LLT cells were washed 3 times with cold PBS buffer, trypsinized and harvested in 0.3 ml PBS buffer. Mean fluorescence intensity of coumarin was analyzed using a FACScan flow cytometer (BD Biosciences, NJ) with 1×10^4 cells collected. Each assay was repeated in triplicate.

LLT cells were seeded in 6-well culture plates (4×10^5 cells/well) and incubated at 37 °C for 24 h. Then, four types of coumarin-labelled micelles were added into the well at a concentration of 2 μM coumarin, and blank control was treated with blank micelles. After incubation for another 3 h, LLT cells were washed 3 times with cold PBS buffer and fixed by 4% paraformaldehyde for 10 min. To visualize the cell nucleus, the cells were stained with Hoechst 33258 (Invitrogen, Beijing, China) in the darkness for 5 min. Finally, the fluorescent signals in LLT cells were imaged by the fluorescent microscopy (Ti-Eclipse, Nikon, Japan).

Destructive effects on VM channels

To appraise the destructive effects of the varying micellar formulations on VM channels, a Matrigel-based tube formation assay was performed. Briefly, Matrigel was placed on an ice box and added into 96-well culture plates (50 μL/well). After incubation at 37 °C for 30 min. LLT cells were digested by trypsin, suspended with serum-free DMEM and inoculated onto the solidified Matrigel (200 μL/well). Then, the varying micelles were separately added into the incubation system. The final concentration of paclitaxel was 10 μM (paclitaxel/honokiol = 1:1, mass ratio). Blank micelles was used as blank control. After incubation for another 4 h, the forming degree of VM channels was monitored and photographed using an inverted microscope (XDS-1B; Chongqing Photoelectric Co., Ltd., Chongqing, China).

Blocking effects on LLT cells invasion

LLT cells invasion assay in vitro was carried out in a 12-well Transwell (Costar, MA). Briefly, LLT cells were digested with 0.25% trypsin and added into the upper chamber of a Transwell chamber (1×10^5 cells/compartment) containing 200 μL of serum-free culture medium. Then, LLT cells were incubated with the varying micellar formulations at a concentration of 10 μM paclitaxel. As a chemoattractant, 600 μL

DMEM containing 10% FBS was added into each lower chamber. After incubation for 8 h, the non-invasion cells in the upper chamber were removed by a cotton swab and the invasion cells were fixed with ice-cold 4% formaldehyde for 30 min, stained with 0.1% crystal violet for 20 min. The quantity of the invasive LLT cells on the lower surface was detected and photographed from three random fields using an inverted microscopy.

To further evaluate inhibitory effects of the varying micellar formulations on LLT cells invasion, a wound-healing assay was also performed *in vitro* according to our previous report [25]. Firstly, LLT cells were planted into in 6-well culture plates (2×10^5 cells/well) and cultured overnight for adherence. After the cells spread to about 60% confluence, a wound scratch was made across the center of well by a sterile pipette tip. Then, cell debris were swilled out using PBS buffer and followed by addition of varying micellar formulations in the wells with a concentration of 10 μM paclitaxel. Blank micelles was used as blank control. Finally, LLT cells were incubated at 37 °C with 5% CO_2 and all scratch area was photographed at 0, 12 and 24 h using an inverted microscopy. Inhibition ratio of wound healing was calculated using the following formula: inhibition ratio $\% = W_{24}/W_0$. W_{24} and W_0 represent the wound width measured by plotting scale in different drug groups at 24 h and 0 h, respectively.

Cell adhesion assay

In the adhesion assay, it was necessary to avoid the bias induced by distinct cytotoxicity. Hence, a SRB staining method was used to evaluate the cytotoxic effects on LLT cells after treatments with the varying micellar formulations for only 12 h with the concentration range of 0–10 μM paclitaxel. Briefly, LLT cells were seeded in 6-well culture plates (1×10^6 cells/well) and incubated at 37 °C for 24 h. The stale medium were removed and fresh DMED medium containing the varying micellar formulations was added into the wells with a concentration of 10 μM paclitaxel, and blank micelles was used as blank control. After incubation for 12 h, LLT cells were digested by trypsin and added into 96-well culture plates which were pre-coated with dilute Matrigel (50 μL per well) at room temperature. After incubation for another 2 h, a SRB staining method was used to evaluate the blocking effects on LLT cell adhesion. The adhesion rate was calculated by the following formula: rate $\% = (A_{540}$ nm for treated groups/A_{540} nm for control group) $\times 100\%$, where A_{540} nm represented the absorbance value measured at 540 nm. Three duplicate wells were set up for each group.

Apoptotic effects to LLT cells

An Annexin V-FITC/propidium iodide (PI) double staining method was used to study the apoptosis inducing effects of the varying formulations to LLT cells. Briefly, LLT cells were seeded into 6-well culture plates (1×10^6 cells/well) at 37 °C for 24 h. Then, the varying micellar formulations were added into wells at a concentration of 10 μM paclitaxel, including

paclitaxel micelles, DQA modified paclitaxel micelles, paclitaxel plus honokiol micelles and DQA modified paclitaxel plus honokiol micelles. Blank micelles was used as blank control. After incubation for another 24 h, LLT cells were trypsinized, harvested and resuspended in binding buffer. The suspension of LLT cells was stained with Annexin V-FITC and PI according to the manufacturer's instructions. After incubation for 10 min at room temperature in the darkness, a FACScan flow cytometer was used to measure the apoptotic effects and plot the apoptotic quadrantal diagram. Each assay was repeated in triplicate.

Regulating effects on metastasis-related protein and apoptotic enzyme

An enzyme-linked immunosorbent assay kit (Cusabio Biotech Co. Ltd., Beijing, China) was used to evaluate the expressions of focal adhesion kinase (FAK), phosphatidylinositol 3-kinase (PI3K), matrix metalloproteinase 2 (MMP-2), matrix metalloproteinase 9 (MMP-9), apoptotic enzyme caspase-9 and caspase-3 in LLT cells. In short, LLT cells were incubated to about 70% confluence and then treated with the varying micelles at a concentration of 10 μM paclitaxel, respectively. Blank micelles was used as blank control. After culture for 12 h, LLT cells were collected and lysed. The acquisition was centrifuged (10,000 rpm) at 4 °C for 15 min. The samples were operated according to the manufacturer's instructions of the kits and analysed by using a microplate reader at 450 nm. Total protein concentrations were analysed by a bicinchoninic acid kit at 540 nm. The protein expression ratio was calculated by the following formula: expression ratio $\% = (A_{450}$ for treated groups/A_{540} for treated groups)/(A_{450} for the control groups/A_{540} for the control groups), where A_{450} and A_{540} were the absorbance values of samples at 450 nm and 540 nm. Each assay was repeated in triplicate.

In vivo *imaging and pharmacodynamics study in tumour-bearing mice*

A non-invasive optical imaging system was used to monitor real-time distributive ability of drug-loaded micelles in xenograft tumour-bearing mice. As a fluorescence probe, fluorescent DiR dye was encapsulated into the micelles. Tumour-bearing mice were established according to our previous report [26]. Briefly, 5×10^6 LLT cells were suspended in 200 μL DMEM medium and implanted in C57BL/6 mice by right antebrachial oxter injection. The mice were cultured under standard laboratory conditions. After tumour volume grew about 400 mm^3, mice were administered with saline, DiR micelles, DQA modified DiR micelles and DQA modified DiR plus honokiol micelles (200 μg/kg) via the tail vein (3 per group). An *in vivo* image system (Carestream FX PRO; Carestream Health Inc., Rochester, NY) was used to scan the anaesthetized mice at 1, 3, 6, 12 and 24 h.

Tumour-bearing mice model was established by inoculating LLT cells in C57BL/6 mice as mentioned above. After 10 days post-inoculation, tumour-bearing mice were randomly distributed into 5 groups and administrated with

physiological saline (blank control), free paclitaxel, paclitaxel micelles, paclitaxel plus honokiol micelles and DQA modified paclitaxel plus honokiol micelles via tail intravenous injection, respectively. The dosage was 3 mg/kg paclitaxel and the treatments were implemented every other day for 4 times in succession. To evaluate the anticancer efficacy of the micellar formulations, tumour size was measured at different points in time by a vernier caliper. Tumour volume ratio was calculated by the following formula: tumour volume ratio = tumour volume measured in each group afterwards/tumour volume measured in each group at day 0. In order to plot the Kaplan–Meier survival curves, survival time was measured from day 10 since inoculation to death and survival rates of tumour-bearing mice were determined every other day. To evaluate the toxicity of the varying micelles, a haematology parameter assay was carried out. Briefly, 20 μL blood samples were drawn from eye sockets of tumour-bearing mice on day 20 after inoculation and sent to a MEK-6318K Hematology Analyzer (Nihon Kohden, Japan) for haematology parameters assay.

Statistical analysis

The data were represented as means ± standard deviations. Analysis of variance was used to determine the significance among groups. A value of $p < .05$ was considered to be significant.

Results

Synthesis of targeting molecule

Figure 1 shows the MALDI-TOF-MS spectra of DSPE-PEG$_{2000}$-NHS (Figure 1(A)) and DSPE-PEG$_{2000}$-DQA (Figure 1(B)). From the spectra, the average mass values of DSPE-PEG$_{2000}$-NHS and DSPE-PEG$_{2000}$-DQA were 2844.31 and 3254.66, respectively. The difference of mass values between the two molecules was corresponded to the mass of DQA, which testified that the targeting molecule was synthesized successfully.
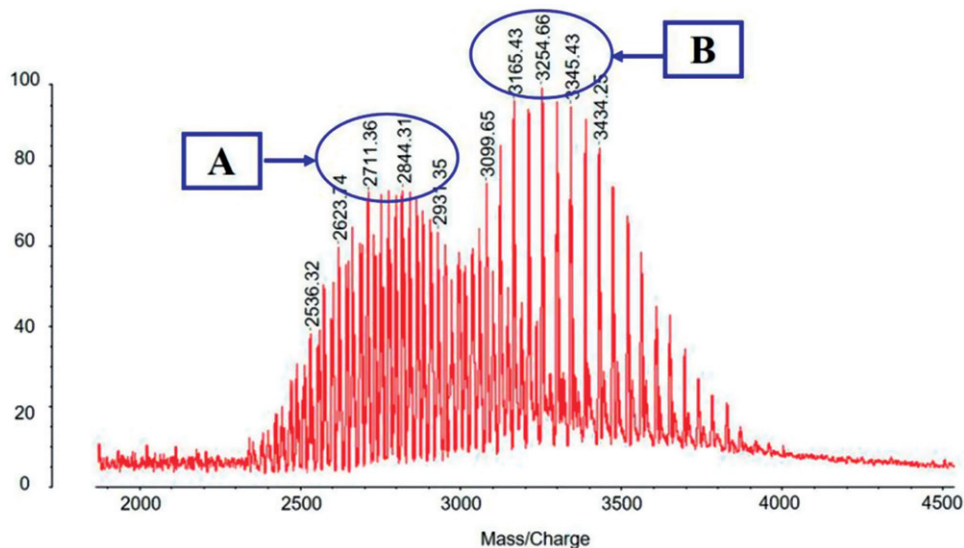
Characterization of the micelles

Figure 2 shows the characterization of DQA modified paclitaxel plus honokiol micelles. According to Figure 2(A), the targeting micelles were mainly composed of soluplus and TPGS$_{1000}$, paclitaxel and honokiol were entrapped simultaneously into the hydrophobic core of the micelles and the functional part of DSPE-PEG$_{2000}$-DQA was exposed outside of the micelles to interact with LLT cells. Results from TEM attested that the morphology of DQA modified paclitaxel plus honokiol micelles was basically spherical (Figure 2(B)). The targeting micelles were monodisperse and about 90 nm in diameter (Figure 2(C)). Table 1 shows the encapsulation efficiencies, particle sizes and polydispersity indexes of the varying micelles. Results illustrated that the encapsulation efficiencies of paclitaxel and honokiol in the varying micellar formulations were greater than 89.00%. The average particle sizes of DQA modified paclitaxel plus honokiol micelles were 91.22 ± 2.19 nm with narrow polydispersity indexes (<0.20). Figure 2(D,E) show the in vitro release rate of paclitaxel and honokiol in PBS solution containing 10% FBS. For DQA modified paclitaxel plus honokiol micelles, the release rates at 48 h were 16.10 ± 1.83% for paclitaxel and 15.83 ± 2.46% for honokiol in PBS solution.

Cytotoxic effects on LLT cells

Figure 3(A) exhibits the inhibitory effects of free drug on LLT cells. Results illustrated that honokiol alone had negligible cytotoxicity on LLT cells, and the survival rate of LLT cells significantly decreased after treatment with the mixture of free drugs consisting of equal paclitaxel and honokiol. The CI values were 0.81 ± 0.06, 0.49 ± 0.05 and 0.57 ± 0.09 for the group of 1:0.5, 1:1 and 1:3, respectively. Therefore, the final proportion of paclitaxel and honokiol was 1:1 (mass ratio) to prepare drug-loaded micelles. Figure 3(B) exhibits the cytotoxic effects on LLT cells after treatment with the varying micellar formulations. Results showed that the cytotoxic effects of DQA modified paclitaxel plus honokiol micelles on LLT cells were the

Figure 1. Characterization of targeting molecular materials. (A) MALDI-TOF-MS spectrum of DSPE-PEG$_{2000}$-NHS, (B) MALDI-TOF-MS spectrum of DSPE-PEG$_{2000}$-DQA.
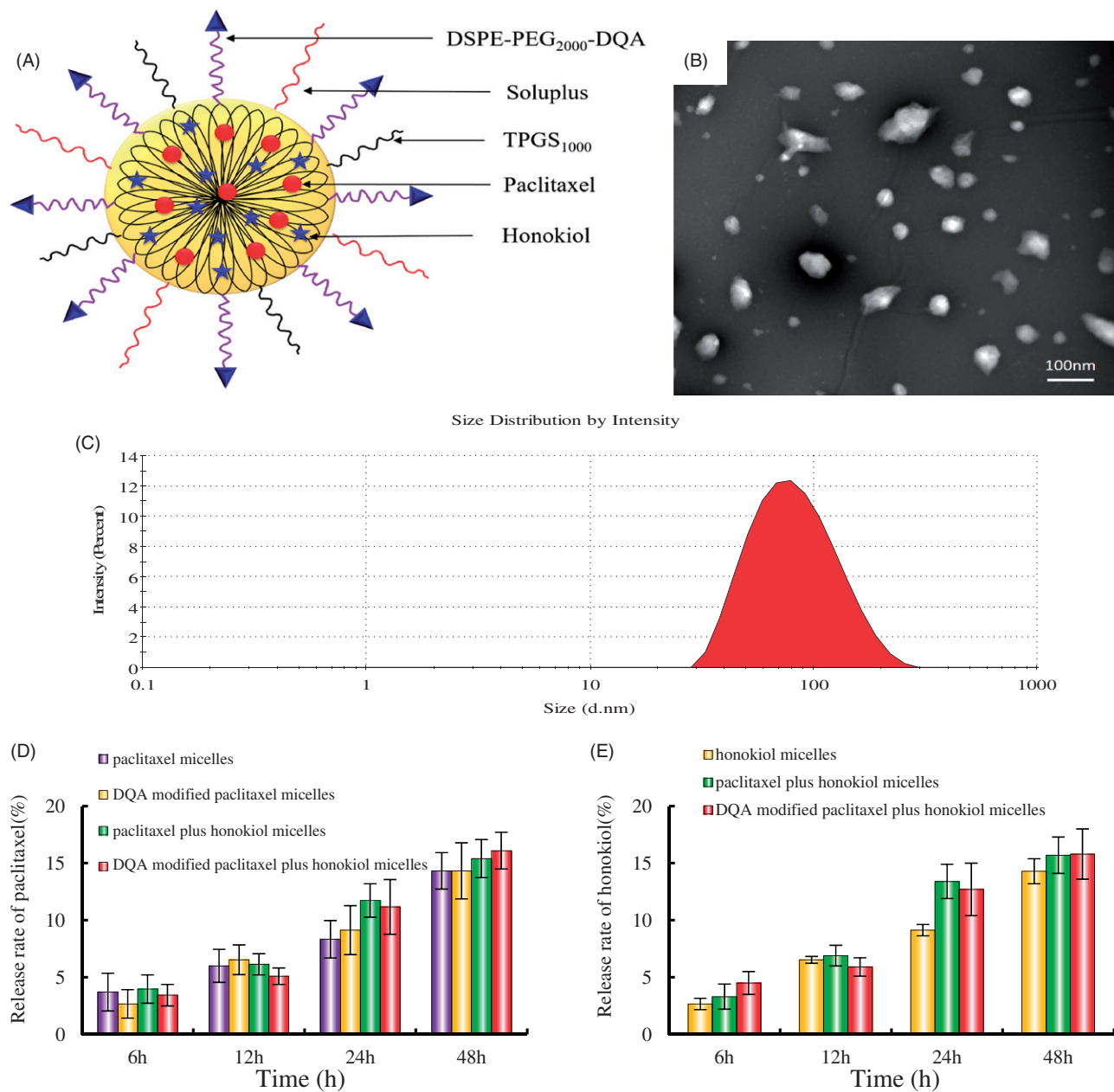
Figure 2. Characterization of DQA modified paclitaxel plus honokiol micelles and release rate of paclitaxel and honokiol in PBS solution containing 10% mouse plasma. (A) A schematic representative of DQA modified paclitaxel plus honokiol micelles, (B) TEM image of DQA modified paclitaxel plus honokiol micelles, agnification × 50,000, (C) Partical size of DQA modified paclitaxel plus honokiol micelles, (D) Release rate of paclitaxel from the varying formulations, € Release rate of honokiol from the varying formulations. Data are presented as mean ± SD ($n = 3$).

Table 1. Characterization of micelles.

	Encapsulation efficiency (%)		Particle size (nm)	PDI
	Paclitaxel	Honokiol		
paclitaxel micelles	96.02 ± 3.26	–	82.43 ± 2.12	0.18 ± 0.01
DQA modified paclitaxel micelles	90.65 ± 3.89	–	87.66 ± 3.28	0.19 ± 0.01
paclitaxel plus honokiol micelles	90.33 ± 3.12	96.89 ± 2.33	84.93 ± 2.98	0.19 ± 0.00
DQA modified paclitaxel plus honokiol micelles	93.27 ± 2.88	89.75 ± 2.62	91.22 ± 2.19	0.17 ± 0.01

strongest among all the groups and blank micelles had minimal cytotoxic effect. The IC$_{50}$ values were 0.16 ± 0.07 for DQA modified paclitaxel plus honokiol micelles, 0.34 ± 0.08 for paclitaxel plus honokiol micelles, 0.61 ± 0.20 for DQA modified paclitaxel micelles and 1.89 ± 0.26 for paclitaxel micelles, respectively.

Cellular uptake and targeting effects in LLT cells

LLT cells were incubated with the varying micellar formulations to evaluate the cellular uptake and targeting effects. Cellular uptake of the micelles was measured by flow cytometry (Figure 4(A,B)). The semiquantitative results illustrated that
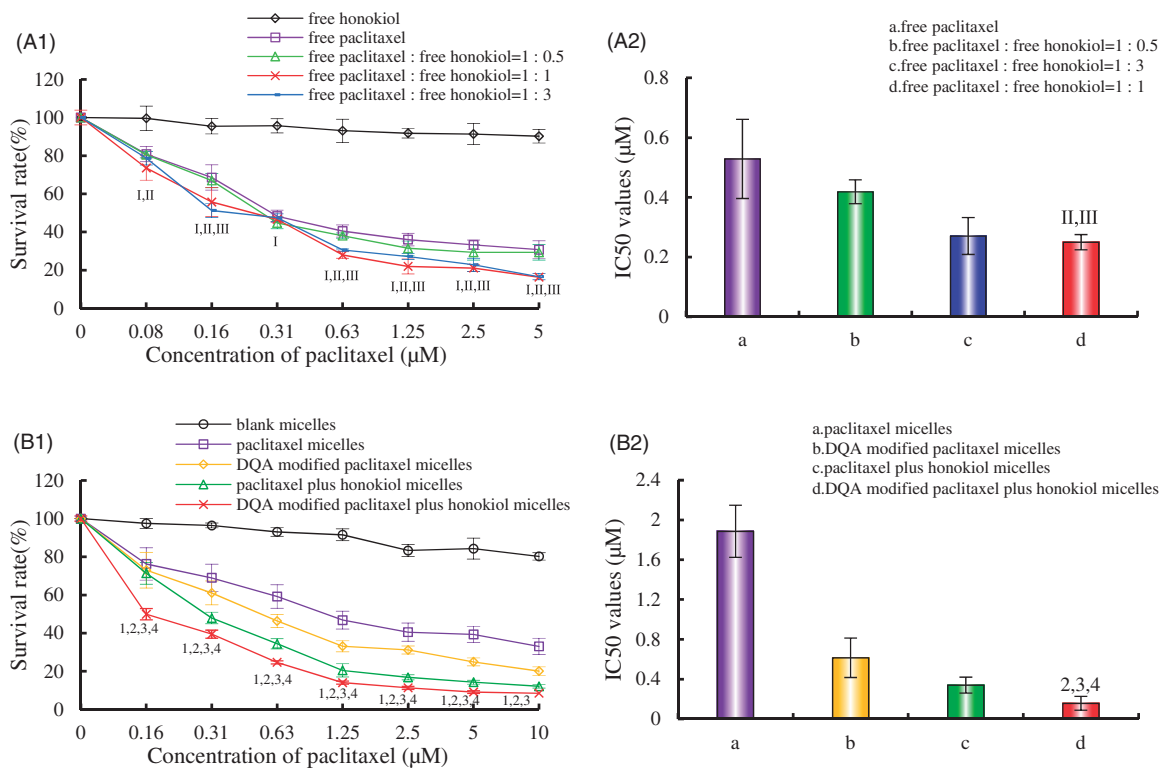
Figure 3. Inhibitory effects on LLT cells after treatments with the varying formulations. (A) Inhibitory effects of free drugs, a, vs. free honokiol; b, vs. free paclitaxel; c, vs. free paclitaxel : free honokiol = 1 : 0.5; d, vs. free paclitaxel : free honokiol = 1 : 1; e, vs. free paclitaxel : free honokiol = 1 : 3. I, vs. a; II, vs. b; III, vs. c; IV, vs. d. (B) Inhibitory effects of micellar formulations. a, vs. blank micelles; b, vs. paclitaxel micelles; c, vs. DQA modified paclitaxel micelles; d, vs. paclitaxel plus honokiol micelles; e, vs. DQA modified paclitaxel plus honokiol micelles. 1, vs. a; 2, vs. b; 3, vs. c; 4, vs. d. Data are presented as mean ± SD ($n = 3$). $p < .05$.

the geometric mean fluorescent intensity values in LLT cells were 3.31 ± 0.66 for blank control, 64.88 ± 6.12 for coumarin micelles, 101.21 ± 10.05 for DQA modified coumarin micelles, 93.43 ± 12.03 for coumarin plus honokiol micelles and 120.31 ± 14.11 for DQA modified coumarin plus honokiol micelles. Figure 4(C) shows the fluorescence images of coumarin in LLT cells. The fluorescence microscopy images illustrated that the fluorescence signal rank in LLT cells was DQA modified coumarin plus honokiol micelles > DQA modified coumarin micelles > coumarin plus honokiol micelles > coumarin micelles > blank micelles.

Destructive effects on VM channels

Figure 5 depicts the destructive effects on VM channels after treatment with the varying micellar formulations. Results showed that LLT cells generated a type of apparent vessel-like networks after being transplanted to the Matrigel. Both DQA modified paclitaxel plus honokiol micelles and paclitaxel plus honokiol micelles exhibited obvious destructive effects on VM channels, and negligible damage was observed after treatment with paclitaxel micelles and DQA modified paclitaxel micelles.

Blocking effects on LLT cells invasion

Figure 6(A) exhibits the blocking effects on LLT cells invasion after treatment with the varying micellar formulations. The intensity of purple signal referred to the numbers of LLT cells which had crossed the membrane of Transwell. Compared

with control group, both DQA modified paclitaxel plus honokiol micelles and paclitaxel plus honokiol micelles exhibited the significant blocking effects on LLT cells invasion. The blocking effects on wound healing after treatment with the varying micellar formulations are exhibited in Figure 6(B). Results showed that the extent of recovery of damaged areas was high after treatment with blank micelles at 12 h and 24 h compared with the initial wound scratch at 0 h. In contrast, Figure 6(C) showed that the inhibition ratio of wound healing of the DQA modified paclitaxel plus honokiol micelles and paclitaxel plus honokiol micelles were $87.4 \pm 7.8\%$ and $77.3 \pm 5.6\%$, respectively, which exhibited the strong blocking effects on wound healing of LLT cells at 12 and 24 h.

Cell adhesion assay

Figure 7 exhibits the adhesion rates of LLT cells on Matrigel. The survival rates of LLT cells were evaluated to eliminate the cytotoxic influence of paclitaxel (Figure 7(A)). Results illustrated that all micellar formulations had negligible cytotoxic effects on LLT cells at a concentration of 10 μM paclitaxel at 12 h, and the survival rate of LLT cells was $90.86 \pm 2.06\%$ after treatment with DQA modified paclitaxel plus honokiol micelles for 12 h. Figure 7(B) shows the adhesion rate of LLT cells after treatment with the varying micellar formulations. The adhesion rate values in LLT cells after treatment with blank micelles, paclitaxel micelles, DQA modified paclitaxel micelles, paclitaxel plus honokiol micelles and DQA modified paclitaxel plus honokiol micelles were $98.16 \pm 3.35\%$, $89.46 \pm 1.86\%$, $97.32 \pm 6.31\%$, $17.61 \pm 0.85\%$ and $16.65 \pm 0.59\%$,
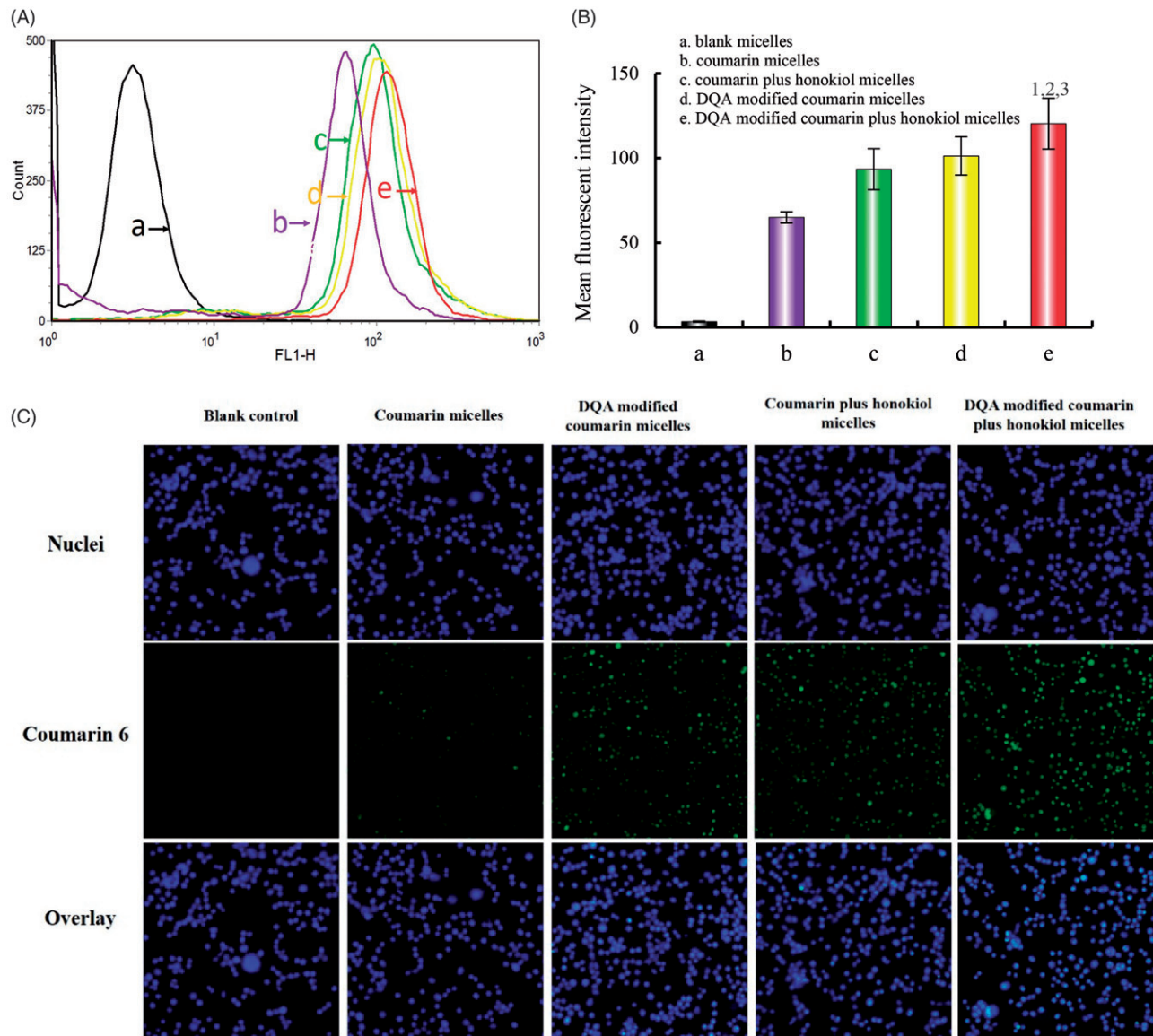
Figure 4. Cellular uptake and targeting effects after incubation with the varying formulations. (A) Cellular uptake of LLT cells, (B) Fluorescence intensity of coumarin 6 in LLT cells, (C) Fluorescence microscopy images of LLT cells incubated with the varying formulations, magnification × 250. a. blank micelles; b. coumarin micelles; c. coumarin plus honokiol micelles; d. DQA modified coumarin micelles; e. DQA modified coumarin plus honokiol micelles. $p < .05$, 1, vs. a; 2, vs. b; 3, vs. c.

respectively. Compared with control group, the adhesion rate was dramatically reduced by 81.51% after treatment with DQA modified paclitaxel plus honokiol micelles.

Apoptotic effects to LLT cells

Figure 8(A) shows the apoptosis inducing effects on LLT cells measured by flow cytometry. The proportion of early and late apoptotic cells was used to evaluate the apoptosis inducing effects of the varying micellar formulations on LLT cells. Results illustrated that LLT cells treated with blank micelles exhibited negligible apoptosis. According to Figure 8(B), the total percentages of apoptosis in LLT cells were $4.22 \pm 0.83\%$ for blank control, $22.96 \pm 0.77\%$ for paclitaxel micelles, $28.46 \pm 2.09\%$ for DQA modified paclitaxel micelles, $24.16 \pm 2.41\%$ for paclitaxel plus honokiol micelles and $29.44 \pm 1.95\%$ for DQA modified paclitaxel plus honokiol micelles, respectively. Under the same drug concentration,

DQA modified paclitaxel plus honokiol micelles had the strongest apoptosis inducing effects on LLT cells.

Regulating effects on metastasis related protein and apoptotic enzyme

Figure 9 illustrates the expressions of four metastasis related proteins (FAK, PI3K, MMP-2 and MMP-9) and two apoptotic enzymes (caspase-9 and caspase-3) in LLT cells after treatment with the varying micellar formulations. Results showed that all metastasis related proteins in LLT cells were obviously down-regulated after treatment with honokiol loaded micelles. For DQA modified paclitaxel plus honokiol micelles, the expressions were down-regulated to 0.72 ± 0.05 for FAK, 0.68 ± 0.12 for PI3K, 0.57 ± 0.11 for MMP-2 and 0.84 ± 0.02 for MMP-9, respectively. In the two groups of apoptotic enzymes, the expression ratios of caspase-9 were enhanced to 1.43 ± 0.09 folds for paclitaxel micelles, 1.54 ± 0.12 folds for
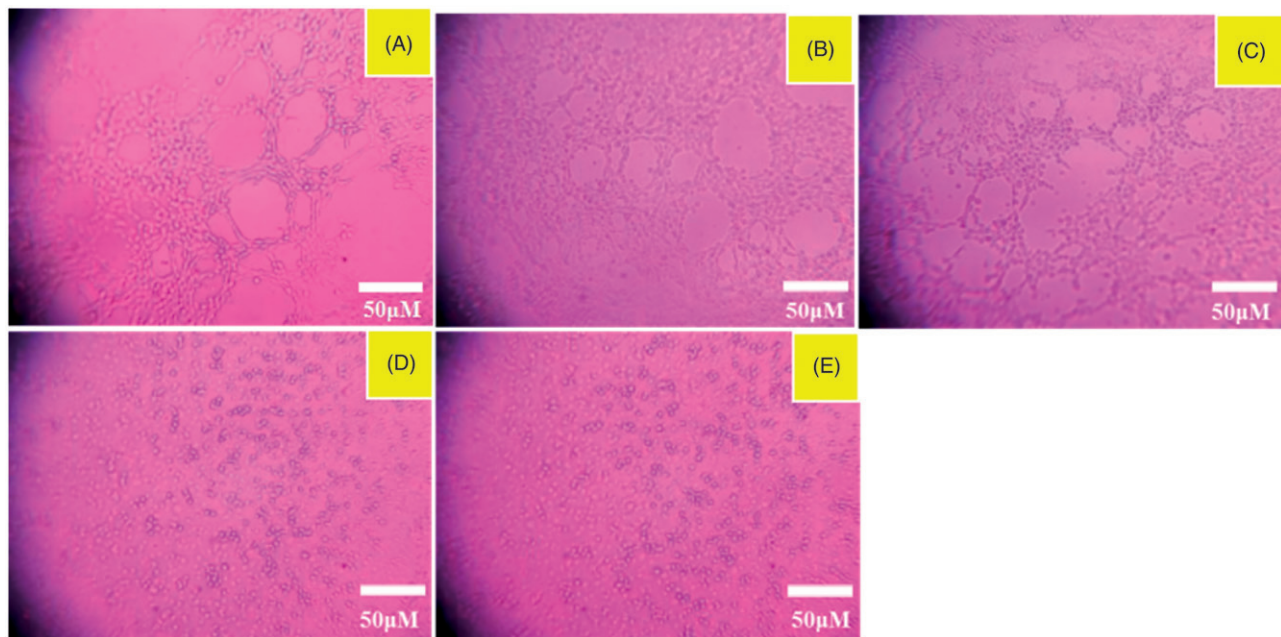
Figure 5. Destructive effects on VM channels after treatments with the varying formulations. a. blank micelles; b. paclitaxel micelles; c. DQA modified paclitaxel micelles; d. paclitaxel plus honokiol micelles; e. DQA modified paclitaxel plus honokiol micelles.

DQA modified paclitaxel micelles, 2.05 ± 0.21 folds for paclitaxel plus honokiol micelles and 2.11 ± 0.12 folds for DQA modified paclitaxel plus honokiol micelles, respectively, and those of caspase-3 were enhanced to 1.17 ± 0.17 folds for paclitaxel micelles, 1.36 ± 0.19 folds for DQA modified paclitaxel micelles, 1.73 ± 0.06 folds for paclitaxel plus honokiol micelles and 1.82 ± 0.15 folds for DQA modified paclitaxel plus honokiol micelles, respectively.

In vivo imaging and pharmacodynamics study in tumour-bearing mice

Figure 10 depicts the *in vivo* real-time imaging in tumor-bearing mice after intravenous administration of the varying DiR micelles. Results showed that strong fluorescent signals were observed in tumor location after the administration of DQA modified DiR plus honokiol micelles and the signals were maintained up to 24 h. Among the formulations, the rank of DiR fluorescent signal at varying time-point was DQA modified DiR plus honokiol micelles > DQA modified DiR micelles > DiR micelles > blank control. Figure 11(A) shows body weight changes of tumor-bearing mice. Results showed that the body weight of mice in treatment groups showed no obvious decline compared with those of normal saline group. Figure 11(B) shows tumour volume changes of tumour-bearing mice after treatment with the varying micellar formulations. Figure 11(C) indicated that tumour volume ratios were 19.92 ± 3.08 for blank control, 19.40 ± 2.67 for free paclitaxel, 18.06 ± 6.23 for paclitaxel micelles, 15.51 ± 3.05 for paclitaxel plus honokiol micelles and 11.66 ± 3.47 for DQA modified paclitaxel plus honokiol micelles, respectively. Figure 11(D) shows the Kaplan-Meier survival curves of tumour-bearing mice after treatment with the varying micellar formulations. Results exhibited that the survival ranges were 12–29 days for blank control, 13–30 days for free

paclitaxel, 15–41 days for paclitaxel micelles, 14–44 days for paclitaxel plus honokiol micelles and 21–47 days for DQA modified paclitaxel plus honokiol micelles, respectively. Table 2 exhibits the haematology parameters after treatment with the varying micellar formulations. Results showed that there was no statistically significant differences between the experimental groups and control group, which indicated that there was negligible systemic toxicity at the test dose.

Discussion

Lung cancer is a principal danger to human health at present. NSCLC represents a primary subgroup of lung cancer, and it is accompanied by high recurrence rate and mortality rate because of tumour metastasis, VM channels and obvious side-effects caused by conventional chemoradiotherapy [27–29]. Moreover, traditional drug delivery systems offer great resistance to cancer treatment due to the restrictions from poor targeting, short half-life of drugs and destruction to healthy cells. Therefore, it urgently needs to explore a drug delivery strategy to overcome these limitations. With the development of nanotechnology, polymeric micelle system is considered one of the most efficient approaches to improve the solubility of hydrophobic drugs and enhance the drug accumulation in tumour site. Hence, in this study, a kind of DQA modified paclitaxel plus honokiol micelles was developed for treatment of NSCLC.

The ideal physicochemical properties of DQA modified paclitaxel plus honokiol micelles were illustrated on the following aspects: smooth sphere in morphology (Figure 2(B)), uniform particle size distribution (Figure 2(C)), narrow PDI (Table 1), preeminent encapsulation efficiencies (Table 1) and retentive drug release (Figure 2(D,E)). The particle size of the targeting micelles was approximately 90 nm which was beneficial for the passive transport of drugs to tumor tissue
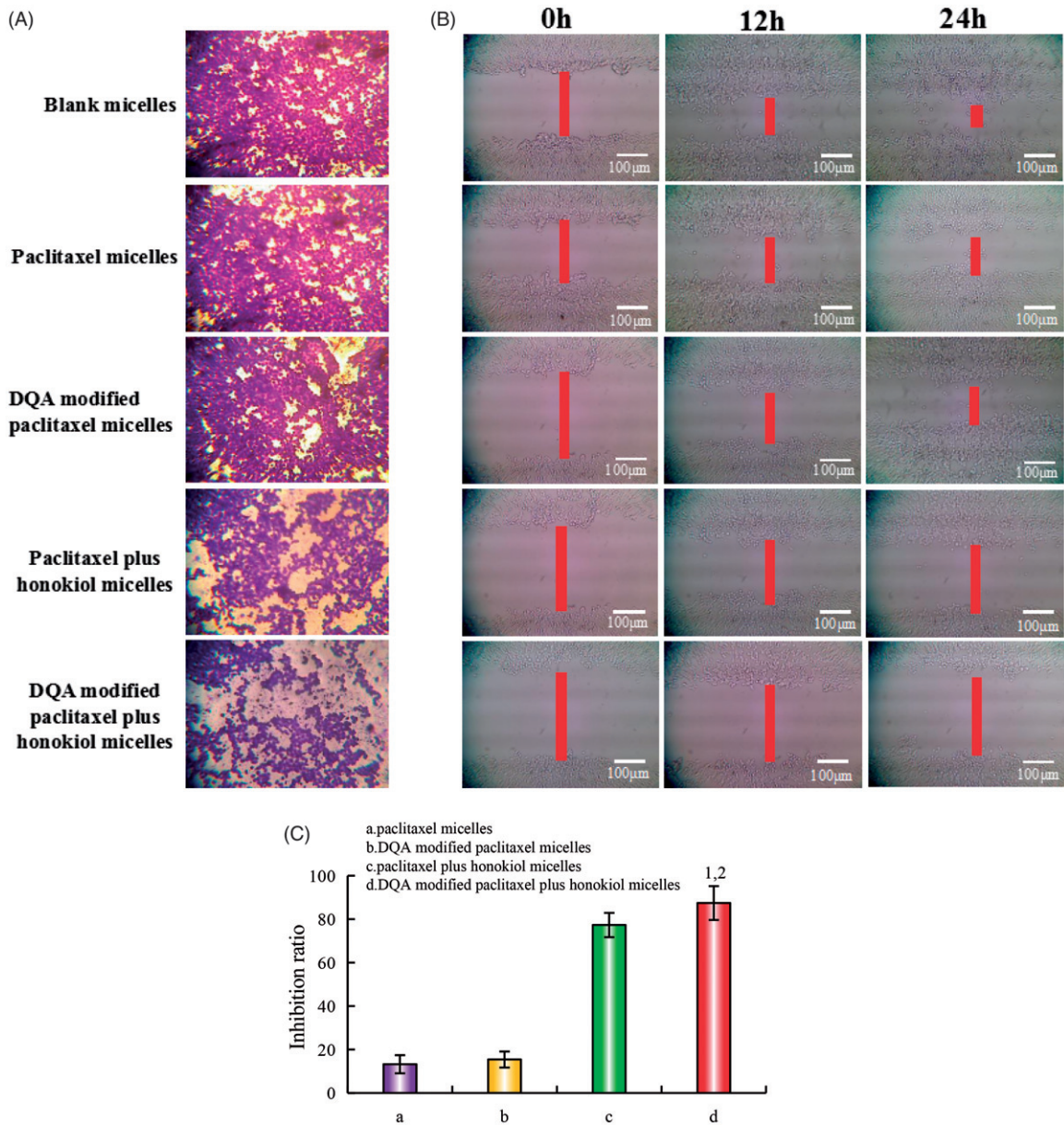
Figure 6. Blocking effects on LLT cells migration and blocking wound healing effects *in vitro* after treatments with the varying micellar formulations. (A) Blocking effects on LLT cells migration, (B) Blocking wound healing effects, C. Inhibition ratio of wound healing. a. paclitaxel micelles; b. DQA modified paclitaxel micelles; c. paclitaxel plus honokiol micelles; d. DQA modified paclitaxel plus honokiol micelles. $p < .05$, 1, vs. a; 2, vs. b; 3, vs. c.
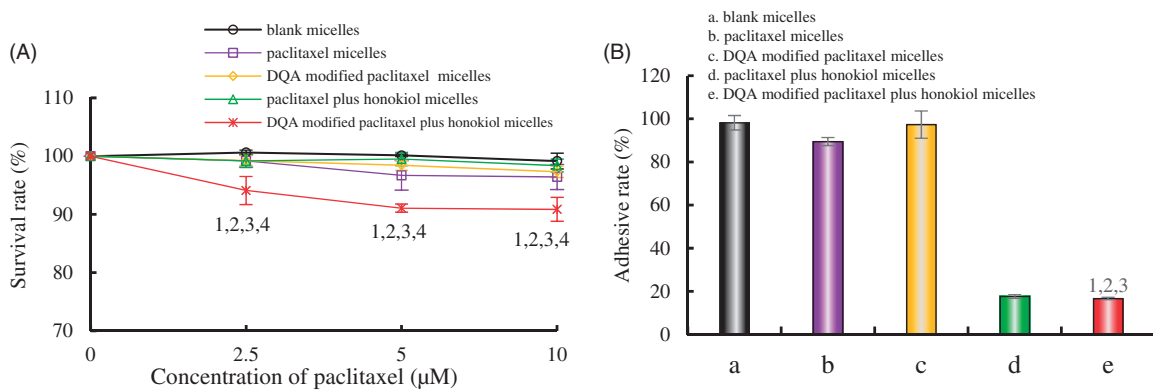

Figure 7. Adhesion rate of LLT cells on Matrigel after incubation with the varying formulations. (A) Cellular survival rate of LLT cells after incubation with drug for 12h, (B) Adhesion rate of LLT cells on Matrigel. a. blank micelles; b. paclitaxel micelles; c. DQA modified paclitaxel micelles; d. paclitaxel plus honokiol micelles; e. DQA modified paclitaxel plus honokiol micelles. $p < .05$, 1, vs. a; 2, vs. b; 3, vs. C; 4, vs. d.

Figure 8. Apoptosis inducing effects on LLT cells after incubation with the varying formulations. (A) Plots by flow cytometry of apoptosis-inducing effects in LLT cells, (B) Apoptosis- inducting effects after treatments with the varying formulations. Data are presented as the mean ± SD (n = 3). a. blank micelles; b. paclitaxel micelless; c. DQA modified paclitaxel micelles; d. paclitaxel plus honokiol micelles; e. DQA modified paclitaxel plus honokiol micelles. $p < .05$, 1, vs. a; 2, vs. b; 3, vs. C; 4, vs. d.
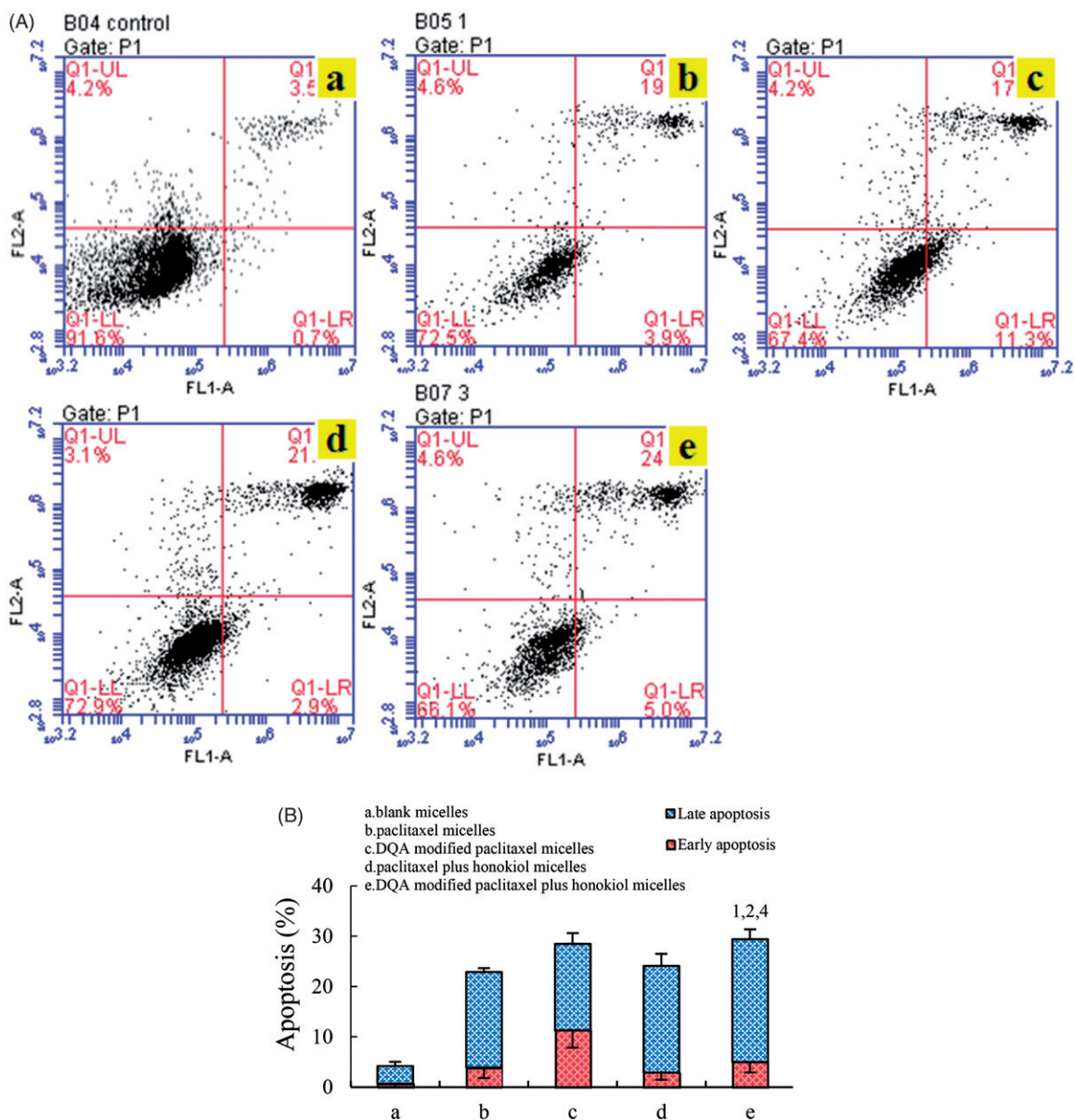
through the leaky vasculature [30]. The high encapsulation efficiencies could increase material utilization and drug delivery efficiency, and the retentive drug release was beneficial for averting drug leakage during the process of drug delivery and increasing drug accumulation in tumour tissue [31].

In this study, coumarin was encapsulated in the inner core of the micelles like paclitaxel and used as a fluorescent probe, and then cellular uptake was evaluated by a flow cytometry (Figure 4(A,B)). Among all micellar formulations, the intracellular fluorescent intensity of coumarin was the highest after treatment with DQA modified coumarin plus honokiol micelles, which indicated that the targeting micelles could increase cellular uptake in LLT cells. Intracellular distributions were ulteriorly evaluated by a fluorescent microscope (Figure 4(C)). LLT cell nucleus was stained by Hoechst 33258 as blue and coumarin was shown as green. Bright blue-green

spots represented the fluorescent signal overlay of coumarin and nucleus. Those results from cellular uptake and colocalization adequately indicated that the modification of DQA on micellar surface could obviously increase the cellular uptake and drug targeting in LLT cells via electrostatic interactions.

To evaluate the inhibitory effects of the varying micellar formulations on LLT cells, cytotoxicity to LLT cells was implemented *in vitro* by a SRB method. Results indicated that the combination of paclitaxel with different concentrations of honokiol exhibited a vigoroso cytotoxicity to LLT cells compared with paclitaxel alone, and honokiol alone had negligible effects on survival rate of LLT cells (Figure 3(A)), which demonstrated that honokiol was instrumental in enhancing therapeutic effect of paclitaxel. Cytotoxicity of micelles on LLT cells was displayed after treatment with the varying micellar formulations (Figure 3(B)). The IC$_{50}$ values of different
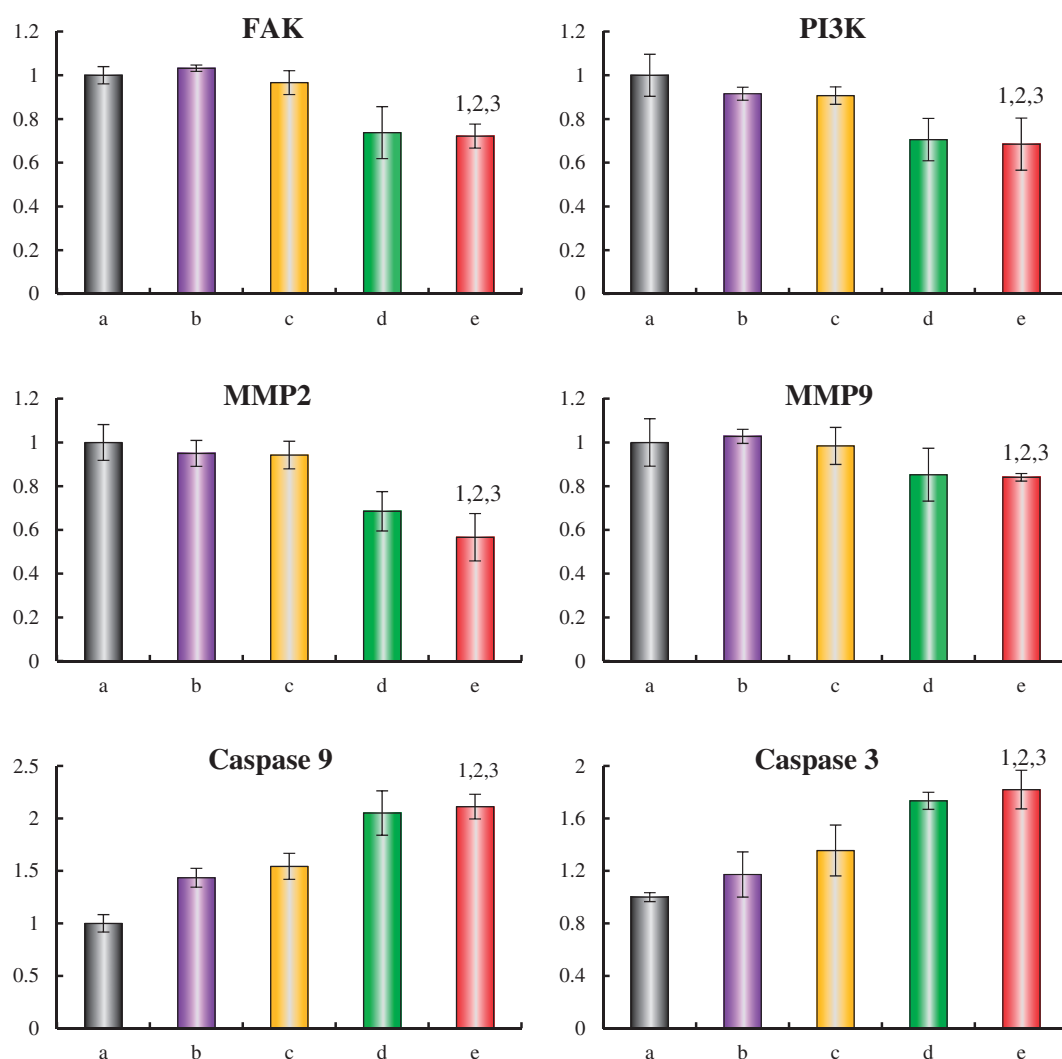
Figure 9. Regulating effects on metastasis related proteins and apoptotic enzyme in LLT cells after treatments with the varying formulations. a. blank micelles; b. paclitaxel micelless; c. DQA modified paclitaxel micelles; d. paclitaxel plus honokiol micelles; e. DQA modified paclitaxel plus honokiol micelles. $p < .05$, 1, vs. a; 2, vs. b; 3, vs. C; 4, vs. d. Data are presented as mean ± SD ($n = 4$).

formulations varied greatly, which was mainly attributed to the addition of honokiol or DQA. It further suggested that the modification of DQA and the existence of honokiol could improve micellar targeting and cytotoxicity to LLT cells.

Cell apoptosis is in connection with a succession of intricate biochemical processes, including membrane permeability change, cell crimp, nuclear collaps and DNA fragmentation [32–34]. To observe apoptosis inducing effects of the varying formulations, an Annexin V-FITC/PI double staining was used to exhibit early and late cell apoptosis after incubation with the varying formulations. As shown in Figure 8, DQA modified paclitaxel plus honokiol micelles displayed the most vigoroso apoptosis inducing effects to LLT cells among all micellar formulations, and this could be due to the activation of apoptotic enzyme by paclitaxel.

In fact, tumour metastasis regulated by multifactor is responsible for 90% of cancer-related mortality [35]. During the course of metastasis, the biochemistry form of the tumour underwent a complicated transformation. Concretely, tumour cells will be partially separated from the primary tumour tissue and adhere to the extracellular matrix after the formation of tumour with sufficient size. Then, tumour cells

acquire the ability of invading to the surrounding tissue. After breaking through the basement membrane into the blood circulation system, tumour cells relocate to the new distal tissues. Subsequently, VM channels were generated under hypoxia by tumour cells to provide adequate nutrition for the rapid growth of tumours before the formation of new blood vessels [36–38]. Therefore, the adhesiveness of tumour cells to extracellular matrix, the invasion ability of tumour cells and the VM channels are the main factors in affecting tumour metastasis.

Reducing the adhesion of tumour cells to extracellular matrix is a necessary strategy for inhibiting tumour metastasis. To evaluate the inhibitory effects on adhesion rate of LLT cells after incubation with the varying micellar formulations, Matrigell was used to imitate extracellular matrix. It was necessary to determine that the micellar concentration used in the adhesion assay should have no effect on the normal survival of LLT cells [39]. As shown in Figure 7(A), all micellar formulations had negligible cytotoxic effects on LLT cells at a concentration of 10 μM paclitaxel which was not enough to suppress the survival of cells within 12 h. Results showed that all honokiol loaded micelles could inhibit the adhesion of LLT
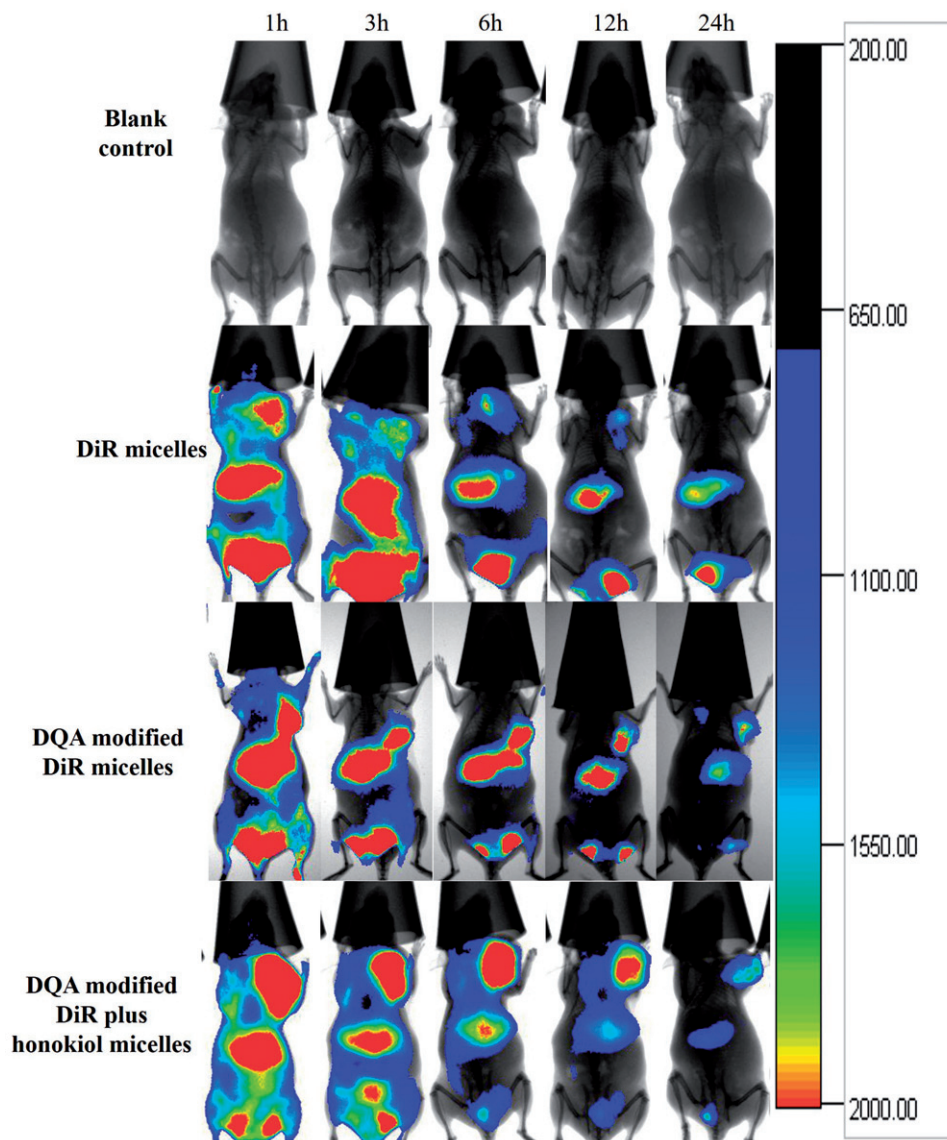
Figure 10. *In vivo* real-time imaging observation after intravenous administration of the varying formulations.

cells to Matrigel and paclitaxel micelles had negligible effect on adhesion rate (Figure 7(B)). For all micellar formulations, DQA modified paclitaxel plus honokiol micelles exhibited the most vigoroso suppression on cell adhesion, which suggested that the targeting micelles could inhibit tumour metastasis in the primary stage.

Invasion is the critical step in tumour metastasis. During the metastatic cascade, tumour cells possessed the ability of invasion break through the basement membrane and give rise to vasculature leakiness, which is essential for tumour cells to penetrate into the blood circulation system [40,41]. To evaluate the inhibitory effects on the invasion of LLT cells after incubation with the varying micellar formulations, the Transwell chambers were established to simulate the basement membrane. Results showed that both paclitaxel plus honokiol micelles and DQA modified paclitaxel plus honokiol micelles had obvious suppression on LLT cell invasion (Figure 6(A)) and the inhibitory effect of paclitaxel micelles and DQA modified paclitaxel micelles were inconspicuous, which suggested that the addition of

honokiol could restrain LLT cells invasion. To further evaluate inhibitory effects of the varying micellar formulations on LLT cells invasion, a wound healing assay was also performed *in vitro*. As showed in Figure 6(B,C), the wound-healing ability of LLT cells without drugs was formidable. In contrast, the strong inhibitory effects were observed after incubation with paclitaxel plus honokiol micelles and DQA modified paclitaxel plus honokiol micelles. Those results further demonstrated that honokiol played a significant role in the process of inhibiting LLT cell invasion.

Under hypoxia concentration, VM channels are generated to provide adequate nutrition for the rapid growth of tumours after tumour cells arrived and were fixed to the distal tissues [38]. Hence, it is necessary to evaluate the ability of destroying VM channels after treatment with the varying micellar formulations. In this study, the VM channel model was established by LLT cells in three-dimensional Matrigel (Figure 5). As shown in the photograph, both paclitaxel plus honokiol micelles and DQA modified paclitaxel plus honokiol micelles exhibited a substantial degree of damage on the VM
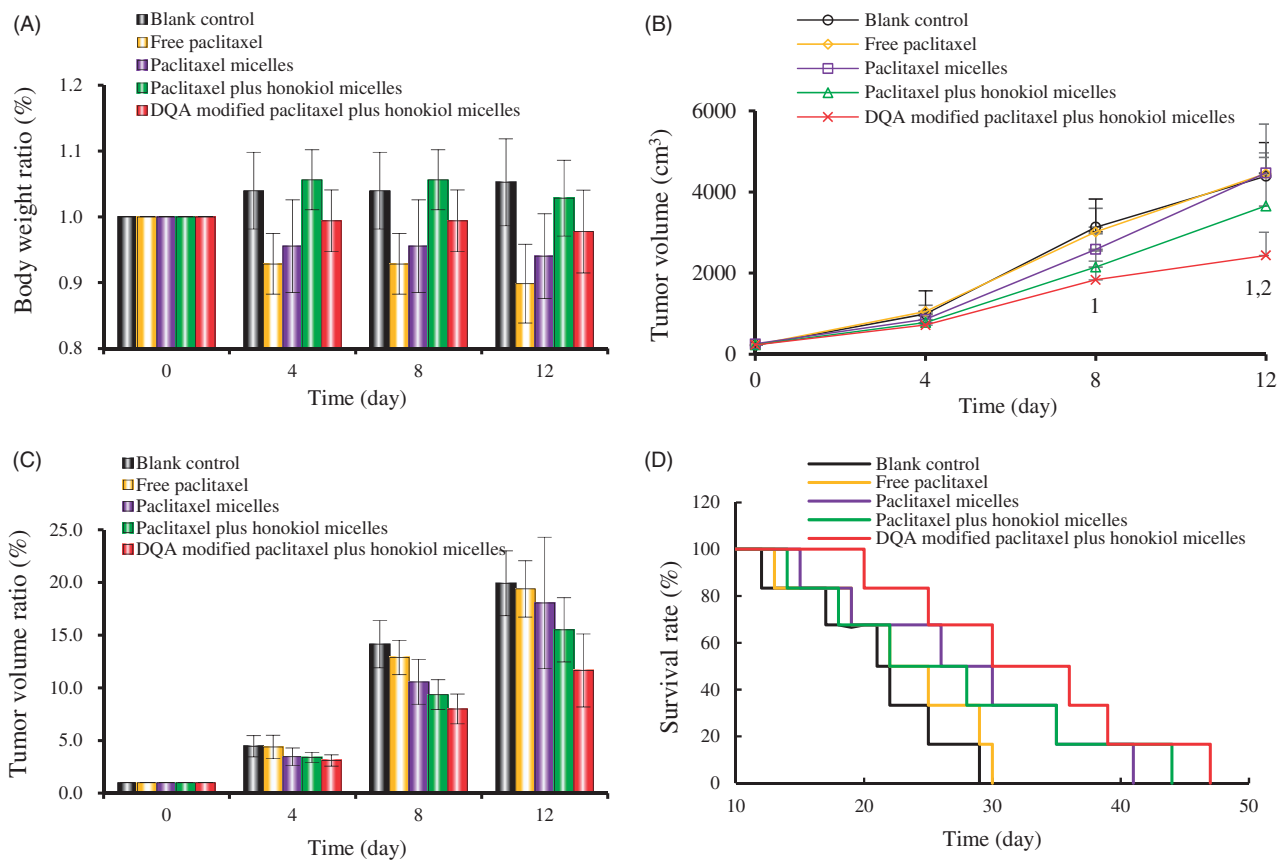
Figure 11. Antitumor effects in LLT cells xenografts mice after treatments with the varying formulations. (A) Body weight changes, (B) Tumour volume, (C) Tumour volume changes, D. Survival rates. 1. blank control; 2. free paclitaxel.

channels, which indicated that the subsistence of honokiol could destroy the VM channels.

Tumour metastasis is originated by numerous variation of related protein expression. FAK, a non-receptor tyrosine kinase, regulates the signals of adhesion and invasion in most cell lines. The over-expression of FAK stimulates tumour cells to acquire the ability of migration. PI3K plays a significant role in facilitating angiogenesis. When tumour cells are activated by over-expressed FAK, cells migrated and reached the distal tissues. Meanwhile, PI3K activated by FAK finally accelerates the formation of VM channels. The interaction of FAK and PI3K impels cell invasion and angiogenesis [42,43]. MMP-2 and MMP-9 can accelerate tumour invasion by degrading the extracellular matrix and the basement membrane [44]. To further evaluate the suppression on tumour metastasis after treatment with the varying micellar formulations, the expression of FAK, PI3K, MMP-2 and MMP-9 were determined using enzyme-linked immunosorbent assay kit. As shown in Figure 9, the expressions of FAK, PI3K, MMP-2 and MMP-9 in LLT cells were obviously decreased after treatment with DQA modified paclitaxel plus honokiol micelles, and this may be the action mechanism for inhibiting tumour metastasis. Apoptosis is a process of programed cell death involved in multicellular organisms. Caspases are a family of protease enzymes which play essential roles in apoptosis. Caspase-9 is an initiator caspase with long pro-domain and caspase-3 is an effector caspase with short pro-domain [45,46]. In this

study, the action mechanism of apoptosis in LLT cells was measured by analysis of apoptotic enzymes. Results showed that two apoptotic enzymes were visibly upregulated by paclitaxel loaded micelles, which may account for the cytotoxicity of paclitaxel.

To observe the distributions of micellar formulations in tumour-bearing mice, the real-time images were captured by entrapping the fluorescent DiR dye into the micelles. As shown in Figure 10, after the administration of DQA modified DiR plus honokiol micelles, strong fluorescent signals still remained in the tumour masses at 24 h, which exhibited a long-circulatory effect and a directed accumulation in tumour location. This could be explained by the combined mechanisms of enhanced permeability and retention (EPR) effect and the targeting effect by the modification of DQA. The pharmacodynamic experiment was carried out on tumour-bearing mice to observe the anticancer effect of the varying micellar formulations. Results showed that the tumour-bearing mice in group of DQA modified paclitaxel plus honokiol micelles exhibited the strongest tumour inhibitory activity and received the longest survival life span compared with other control groups, which indicated that an overall better treatment efficacy had been achieved after treatment with the targeting micelles (Figure 11(B–D)). Body weight ratios and the analysis of haematological parameters attested that there was negligible systemic toxicity after treatment with DQA modified paclitaxel plus honokiol micelles (Figure 11(A) and Table 2).

Table 2. Haematology parameters assay results from tumour-bearing mice.

Assay	Normal saline	Free paclitaxel	Paclitaxel micelles	Paclitaxel plus honokiol micelles	DQA modified paclitaxel plus honokiol micelles
WBC	6.43 ± 1.51	6.50 ± 0.94	7.13 ± 3.32	4.63 ± 1.48	5.98 ± 1.72
RBC	5.20 ± 1.24	8.12 ± 0.84	7.19 ± 3.29	7.14 ± 0.91	6.93 ± 0.69
HGB	139.25 ± 11.03	137.25 ± 20.69	128.50 ± 55.46	143.75 ± 18.30	130.25 ± 9.50
HCT	37.86 ± 5.45	38.65 ± 4.96	35.63 ± 6.01	39.60 ± 10.21	38.85 ± 3.73
MCV	44.28 ± 3.06	43.80 ± 4.61	45.03 ± 7.58	45.70 ± 3.32	43.45 ± 0.93
MCH	16.30 ± 1.37	17.18 ± 1.58	15.38 ± 2.42	15.25 ± 2.47	16.28 ± 0.94
MCHC	349.50 ± 27.53	357.25 ± 16.40	350.50 ± 70.26	346.50 ± 27.89	326.00 ± 30.89
RDW	13.35 ± 1.33	16.65 ± 3.09	15.73 ± 1.66	15.18 ± 4.55	13.23 ± 0.53
PLT	327.00 ± 58.34	402.25 ± 118.74	371.25 ± 41.36	341.25 ± 73.65	329.50 ± 61.91
PCT	0.25 ± 0.08	0.22 ± 0.13	0.24 ± 0.09	0.13 ± 0.08	0.19 ± 0.05
MPV	9.33 ± 5.70	4.10 ± 1.41	6.15 ± 4.33	6.55 ± 4.44	6.13 ± 4.26
PDW	15.53 ± 1.27	14.83 ± 1.67	13.68 ± 1.81	15.55 ± 0.99	14.13 ± 0.96
LYM	1.10 ± 0.39	0.93 ± 0.43	1.00 ± 0.70	0.93 ± 0.49	1.58 ± 0.13
MID	0.60 ± 0.22	0.35 ± 0.13	0.43 ± 0.10	0.93 ± 0.50	0.58 ± 0.39
GRN	4.85 ± 1.16	4.55 ± 2.43	4.93 ± 2.30	3.58 ± 0.88	4.80 ± 0.64
LYM%	13.23 ± 2.78	13.73 ± 9.24	20.50 ± 3.23	20.75 ± 3.04	21.68 ± 3.78
MID%	4.70 ± 1.27	5.65 ± 1.65	3.33 ± 1.49	7.90 ± 3.58	4.30 ± 1.27
GRN%	71.03 ± 4.38	83.95 ± 7.75	75.13 ± 11.61	73.08 ± 15.32	70.15 ± 15.42

Conclusion

In this study, we prepared the DQA modified paclitaxel plus honokiol micelles and evaluated physical characteristics, targeting effect, cytotoxicity, inhibitory effect on tumor metastasis from all angles and anticancer efficacy *in vivo*. The experimental results testified that the targeting micelles prepared in this study were associated with the following characteristics: (i) the ideal particle size ($\sim$90 nm) was more convenient for accumulation in tumour tissue; (ii) the modification of DQA on the surface of micelles was conducive to cellular uptake and improvement of targeting; (iii) the addition of honokiol reduced the adhesion of tumour cells to extracellular matrix, inhibited the invasion of LLT cells and destroyed the VM channels by down-regulating the expression of a variety of proteins. *In vivo* assays showed that the targeting micelles exhibited a conspicuous antitumor efficacy with a negligible systemic toxicity. Therefore, the DQA modified paclitaxel plus honokiol micelles prepared in this study provided a potential treatment strategy for NSCLC.

Disclosure statement

No potential conflict of interest was reported by the authors.

Funding

References

[1] Dubey P, Gidwani B, Pandey R, et al. In vitro and in vivo evaluation of PEGylated nanoparticles of bendamustine for treatment of lung cancer. Artif Cells Nanomed Biotechnol. 2016;44:1491–1497.

[2] Shen J, Wang B, Zhang T, et al. Suppression of non-small cell lung cancer growth and metastasis by a novel small molecular activator of RECK. Cell Physiol Biochem. 2018;45:1807–1817.

[3] Dearing KR, Sangal A, Weiss GJ. Maintaining clarity: review of maintenance therapy in non-small cell lung cancer. World J Clin Oncol. 2014;5:103–113.

[4] Wu H, Zhong Q, Zhong R, et al. Preparation and antitumor evaluation of self-assembling oleanolic acid-loaded Pluronic P105/d-alpha-tocopheryl polyethylene glycol succinate mixed micelles for non-small-cell lung cancer treatment. IJN. 2016;11: 6337–6352.

[5] Zhu Y, Zhu R, Wang M, et al. Anti-metastatic and anti-angiogenic activities of core-shell SiO$_2$@LDH loaded with etoposide in non-small cell lung cancer. Adv Sci (Weinh). 2016;3:1600229

[6] Maniotis AJ, Folberg R, Hess A, et al. Vascular channel formation by human melanoma cells in vivo and in vitro: vasculogenic mimicry. Am J Pathol. 1999;155:739–752.

[7] Li Y, Sun B, Zhao X, et al. MMP-2 and MMP-13 affect vasculogenic mimicry formation in large cell lung cancer. J Cell Mol Med. 2017;21:3741–3751.

[8] Yao L, Zhang D, Zhao X, et al. Dickkopf-1-promoted vasculogenic mimicry in non-small cell lung cancer is associated with EMT and development of a cancer stem-like cell phenotype. J Cell Mol Med. 2016;20:1673–1685.

[9] Perez SA, de Haro C, Vicente C, et al. New acridine thiourea gold(I) anticancer agents: targeting the nucleus and inhibiting vasculogenic mimicry. ACS Chem Biol. 2017;12:1524–1537.

[10] Huo J. Effects of chitosan nanoparticle-mediated BRAF siRNA interference on invasion and metastasis of gastric cancer cells. Artif Cells Nanomed Biotechnol. 2016;44:1232–1235.

[11] Chen X, Fu Y, Xu H, et al. SOX5 predicts poor prognosis in lung adenocarcinoma and promotes tumor metastasis through epithelial-mesenchymal transition. Oncotarget 2018;9:10891–10904.

[12] Buttigliero C, Bertaglia V, Novello S. Anti-angiogenetic therapies for central nervous system metastases from non-small cell lung cancer. Transl Lung Cancer Res. 2016;5:610–627.

[13] Zhang Y, Thayele Purayil H, Black JB, et al. Prostaglandin E2 receptor 4 mediates renal cell carcinoma intravasation and metastasis. Cancer Lett. 2017;391:50–58.

[14] Wang H, Yin H, Yan F, et al. Folate-mediated mitochondrial targeting with doxorubicin-polyrotaxane nanoparticles overcomes multidrug resistance. Oncotarget. 2015;6:2827–2842.

[15] Bae Y, Jung MK, Song SJ, et al. Functional nanosome for enhanced mitochondria-targeted gene delivery and expression. Mitochondrion. 2017;37:27–40.

[16] Shen L, Zhang F, Huang R, et al. Honokiol inhibits bladder cancer cell invasion through repressing SRC-3 expression and epithelial-mesenchymal transition. Oncol Lett. 2017;14:4294–4300.

[17] Singh T, Katiyar SK. Honokiol inhibits non-small cell lung cancer cell migration by targeting PGE$_2$-mediated activation of β-catenin signaling . PLoS One. 2013;8:e60749

[18] Chen X, Sun X, Guan J, et al. Rsf-1 influences the sensitivity of non-small cell lung cancer to paclitaxel by regulating NF-κB pathway and its downstream proteins. Cell Physiol Biochem. 2017;44: 2322–2336.

[19] Zhang L, Liu Z, Yang K, et al. Tumor progression of non-small cell lung cancer controlled by albumin and micellar nanoparticles

of itraconazole, a multitarget angiogenesis inhibitor. Mol Pharmaceutics. 2017;14:4705–4713.

[20] Parent LR, Bakalis E, Ramírez-Hernández A, et al. Directly observing micelle fusion and growth in solution by liquid-cell transmission electron microscopy. J Am Chem Soc. 2017;139:17140–17151.

[21] Zhao J, Xu Y, Wang C, et al. Soluplus/TPGS mixed micelles for dioscin delivery in cancer therapy. Drug Dev Ind Pharm. 2017;43:1197–1204.

[22] Gu Y, Li J, Li Y, et al. Nanomicelles loaded with doxorubicin and curcumin for alleviating multidrug resistance in lung cancer. Int J Nanomedicine. 2016;11:5757–5770.

[23] Song XL, Liu S, Jiang Y, et al. Targeting vincristine plus tetrandrine liposomes modified with DSPE-PEG2000-transferrin in treatment of brain glioma. Eur J Pharm Sci. 2017;96:129–140.

[24] Szymusiak M, Kalkowski J, Luo H, et al. Core-shell structure and aggregation number of micelles composed of amphiphilic block copolymers and amphiphilic heterografted polymer brushes determined by small-angle X-ray scattering. ACS Macro Lett. 2017;6:1005–1012.

[25] Li XT, Zhou ZY, Jiang Y, et al. PEGylated VRB plus quinacrine cationic liposomes for treating non-small cell lung cancer. J Drug Target. 2015;23:232–243.

[26] Li XT, He ML, Zhou ZY, et al. The antitumor activity of PNA modified vinblastine cationic liposomes on Lewis lung tumor cells: In vitro and in vivo evaluation. Int J Pharm. 2015;487:223–233.

[27] Mei D, Zhao L, Chen B, et al. alpha-Conotoxin ImI-modified polymeric micelles as potential nanocarriers for targeted docetaxel delivery to alpha7-nAChR overexpressed non-small cell lung cancer. Drug Deliv. 2018;25:493–503.

[28] Zhao MH, Yuan L, Meng LY, et al. Quercetin-loaded mixed micelles exhibit enhanced cytotoxic efficacy in non-small cell lung cancer in vitro. Exp Ther Med 2017;14:5503–5508.

[29] Wang D, Lin Y, Gao B, et al. Reduced expression of FADS1 predicts worse prognosis in non-small-cell lung cancer. J Cancer. 2016;7:1226–1232.

[30] Liu Y, Mei L, Yu Q, et al. Multifunctional tandem peptide modified paclitaxel-loaded liposomes for the treatment of vasculogenic mimicry and cancer stem cells in malignant glioma. ACS Appl Mater Interfaces. 2015;7:16792–16801.

[31] Liu Y, Lu WL, Guo J, et al. A potential target associated with both cancer and cancer stem cells: a combination therapy for eradication of breast cancer using vinorelbine stealthy liposomes plus parthenolide stealthy liposomes. J Control Release. 2008;129:18–25.

[32] Li Y, Guo M, Lin Z, et al. Polyethylenimine-functionalized silver nanoparticle-based co-delivery of paclitaxel to induce HepG2 cell apoptosis. IJN. 2016;11:6693–6702.

[33] Yu S, Sheu HM, Lee CH. Solanum incanum extract (SR-T100) induces melanoma cell apoptosis and inhibits established lung metastasis. Oncotarget 2017;8:103509–103517.

[34] Sadat Shandiz SA, Shafiee Ardestani M, Shahbazzadeh D, et al. Novel imatinib-loaded silver nanoparticles for enhanced apoptosis of human breast cancer MCF-7 cells. Artif Cells Nanomed Biotechnol. 2017;45:1–10.

[35] Sun YW, Xu J, Zhou J, et al. Targeted drugs for systemic therapy of lung cancer with brain metastases. Oncotarget 2018;9:5459–5472.

[36] Thakur C, Rapp UR, Rudel T. Cysts mark the early stage of metastatic tumor development in non-small cell lung cancer. Oncotarget. 2018;9:6518–6535.

[37] Glinsky GV. Activation of endogenous human stem cell-associated retroviruses (SCARs) and therapy-resistant phenotypes of malignant tumors. Cancer Lett. 2016;376:347–359.

[38] Schnegg CI, Yang MH, Ghosh SK, et al. Induction of vasculogenic mimicry overrides VEGF-A silencing and enriches stem-like cancer cells in melanoma. Cancer Res. 2015;75:1682–1690.

[39] Hu J, Chen LJ, Liu L, et al. Liposomal honokiol, a potent anti-angiogenesis agent, in combination with radiotherapy produces a synergistic antitumor efficacy without increasing toxicity. Exp Mol Med. 2008;40:617–628.

[40] Wan X, Kong Z, Chu K, et al. Co-expression analysis revealed PTCH1-3'UTR promoted cell migration and invasion by activating miR-101-3p/SLC39A6 axis in non-small cell lung cancer: implicating the novel function of PTCH1. Oncotarget. 2018;9:4798–4813.

[41] Shan Y, Cao W, Wang T, et al. ZNF259 inhibits non-small cell lung cancer cells proliferation and invasion by FAK-AKT signaling. Cancer Manag Res. 2017;9:879–889.

[42] Lu XS, Sun W, Ge CY, et al. Contribution of the PI3K/MMPs/Ln-5gamma2 and EphA2/FAK/Paxillin signaling pathways to tumor growth and vasculogenic mimicry of gallbladder carcinomas. Int J Oncol. 2013;42:2103–2115.

[43] Pylayeva Y, Gillen KM, Gerald W, et al. Ras- and PI3K-dependent breast tumorigenesis in mice and humans requires focal adhesion kinase signaling. J Clin Invest. 2009;119:252–266.

[44] Shen KH, Hung JH, Chang CW, et al. Solasodine inhibits invasion of human lung cancer cell through downregulation of miR-21 and MMPs expression. Chem Biol Interact. 2017;268:129–135.

[45] Liu YR, Sun B, Zhao XL, et al. Basal caspase-3 activity promotes migration, invasion, and vasculogenic mimicry formation of melanoma cells. Melanoma Res. 2013;23:1–253.

[46] Lee NR, Park BS, Kim SY, et al. Cytokine secreted by S100A9 via TLR4 in monocytes delays neutrophil apoptosis by inhibition of caspase 9/3 pathway. Cytokine. 2016;86:53–63.